Phase diagram of the Voronoi model of biological tissue

Author: Oriol Reig Fité
Facultat de Física, Universitat de Barcelona, Diagonal 645, 08028 Barcelona, Spain.

Advisor: Matteo Paoluzzi

Abstract: Recent experiments show a relation between cell's shape and collective motion in confluent monolayers. Collective motion can cause structural changes in biological tissues that can be rationalized within the framework of Voronoi models. Using Monte Carlo method, we have studied the equilibrium properties of the model using as control parameters the typical cell elongation and the intensity of the noise. We have studied the dynamical and structural changes in the tissues, which has let us explore the phase diagram around the solid-to-liquid transition.

I. INTRODUCTION

Collective cell migration is a phenomenon that has been observed in a variety of biological situations, such as wound healing, cancer metastasis or embryogenesis [3, 4, 7, 10]. Recent studies have shown that when cells are heavily packed this motion is mostly due to cell-cell junction, and some transitions might coincide with a collective solid-to-liquid jamming transition [5, 11]. This behaviour, which involves much bigger scales than cell sizes, suggest that a physical model should only count a few parameters [12]. One of the several models that studies this collective cell motility is the Voronoi model, which was first proposed by Honda in [6] and has some strong experimental support [1]. In a Voronoi model, the biological tissue results from the Voronoi tessellation of the cell centers, i.e., the set of points that are closer to the cell's center than to any other cell's center. In this picture, cells are polygons with well-defined areas and perimeters. Because of this construction, this model describes confluent monolayers, where cells are packed without free space. In Voronoi models, it is possible to define a configurational energy, i.e., an energy functional that depends on the geometrical properties of the system, that is expressed as

$$E = \sum_{cells\ i} K_A(A_i - A_0)^2 + K_P(P_i - P_0)^2 \qquad (1)$$

where A_i and P_i are the area and perimeter of the cell i, respectively. The first term is related to the incompressibility in three dimensions as well as the resistance of the layer to height fluctuations, where A_0 behaves as a preferred or target area and K_A is the elastic area constant. The second term corresponds to the competition between cell-cell adhesion and active contractility in the actomyosin cortex, where P_0 and K_P are the analogous of A_0 and K_A, respectively.

Consequently, it is possible to introduce a dimensionless parameter p_0 that is called target shape index and whose definition is

$$p_0 = \frac{P_0}{\sqrt{A_0}}.$$

p_0 is an estimator of the typical cell elongation, geometrically the shape index of a regular hexagon is $p_0^{hex} = 6/\sqrt{3\sqrt{3}/2} \approx 3.722$, and the shape index of a regular pentagon is $p_0^{pent} = 5/\sqrt{1/4 \cdot \sqrt{5(5+2\sqrt{5})}} \approx 3.81$. The energy E given by Eq.(1) can be seen as a cost function that the system tends to minimize. This cost function depends on the shape index p_0 so that is minimized when each cell is a polygon whose shape parameter ($\frac{P_i}{\sqrt{A_i}}$) is p_0. We will call q the mean observed shape parameter:

$$q = \frac{1}{N} \sum_{cells\ i} \frac{P_i}{\sqrt{A_i}}. \qquad (2)$$

Bi *et al.* [1] studied the mechanical energy required to execute T1 transitions in simulated systems, which consist of the shrinking of an edge between two cells until a new edge arises between two neighbouring cells. They concluded that there is a critical value of q, $q^* \approx 3.81$, by which if $q \lesssim q^*$ the system behaves like a solid, whereas if $q \gtrsim q^*$ the system behaves like a liquid. These predictions have been verified by recent experiments on the asthmatic airway epithelium [9].

From now on we set $K_A, K_P, A_0 = 1$, and thus the energy in Eq.(1) can be expressed as

$$E = \sum_{cells\ i} (A_i - 1)^2 + (P_i - p_0)^2. \qquad (3)$$

Furthermore, we can define the effective mechanical interaction over the cell i as $\mathbf{F}_i = -\nabla_i E$, with ∇_i indicating the gradient with respect the cell center $\mathbf{r}_i$. In addition to this force, cells can move because of self-propulsion, i.e., the motion of the cell in the absence of neighbours. Cells achieve self propulsion by extending different types of protrusion and adhering them to their surroundings [12]. We can consider a stochastic force representing cell motion, for example, Bi *et al.* [2] assigned a polarity vector to each cell

$$\hat{\mathbf{n}}_i = (\cos\theta_i, \sin\theta_i) \qquad (4)$$

where the time evolution of θ_i can be represented by a white-noise process (zero mean and finite variance). Along this vector the cell exerts a self-propulsion force of constant magnitude $v_0\mu$, where μ is the mobility.

At low Reynolds numbers (when inertia forces can be neglected) this gives rise to the overdamped equation of motion of each cell center:

$$\frac{d\mathbf{r}_i}{dt} = \mathbf{F}_i + \mathbf{f}_i^s \tag{5}$$

where $\mathbf{f}_i^s$ is the stochastic force, which in our case acts as white noise.

We have studied the phase diagram of the model focusing on two phases, one where the system behaves as a solid and another one where cells move as molecules in the liquid state.

II. MONTE CARLO METHOD

The trajectories of cells centers and therefore the evolution of the system are determined by Eq.(5), which can be solved numerically as in [2]. Another approach is to consider the Monte Carlo dynamics of the energy in Eq.(3). Following [8] we have implemented the Metropolis Monte Carlo method, which works as follows: first the N cells are given a random configuration, i.e., the N cell's center are given random coordinates. Next we perform the Voronoi tessellation of these points and we calculate the energy of the system according to Eq.(3). Now we take a cell center and we move it a certain distance smaller than a fixed dr and in a random direction (with periodic boundary conditions), and we compute the energy of the system in this new configuration. Let $\Delta E := E_n - E_o$ denote the difference between the energy of the previous configuration and the energy of the new one, we accept this trial move with probability

$$P_{acc} \propto \exp(-\beta \Delta E) \tag{6}$$

where $\beta = 1/T$ and T is a control parameter that measures the strength of the noise, i.e., the temperature in the case of an equilibrium system in contact with a thermal bath. We are therefore considering that cells perform a Brownian motion, where T controls the intensity of the random motion as a fluid in a thermal equilibrium at temperature T. The system samples a stationary value of energy after a certain number of Monte Carlo steps, thus the physical observables of the system are computed after this value.

III. SIMULATIONS AND RESULTS

For studying the phase diagram of the system we performed Monte Carlo simulations of a confluent monolayer composed of $N = 100$ cells. For obtaining the stationary properties of the system, we have followed the dynamics for $t_{max} = 10^4$ Monte Carlo (MC) steps. As one can see in Fig.(1) where we report the typical evolution of the energy Eq.(3), the energy converges towards stationary values after an initial transient that is smaller than 100 MC steps. Furthermore, we have fixed the maximum displacement of the cell center in the trial moves of the Monte Carlo method at $dr = 0.25$ (as in [8]). This value cannot be too small, otherwise we are not exploring new configurations, or too large (compared with the typical cell length) so that the energy reaches the minimum quicker.

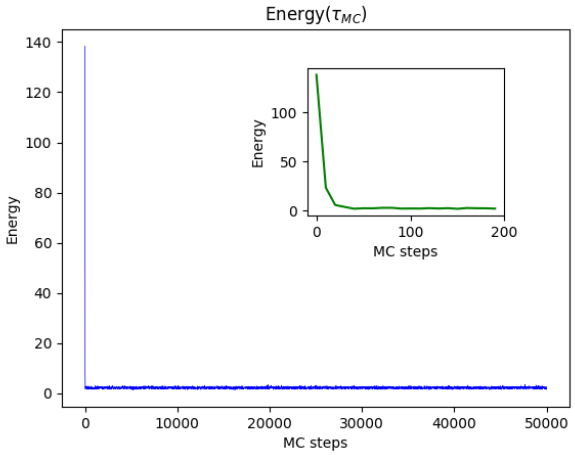

FIG. 1: Evolution of the energy of the system computed with Eq.(3) (in arbitrary units) throughout the simulation, for $5 \cdot 10^4$ MC steps with $T = 0.08$ and $p_0 = 3.4$. We can see that energy quickly reaches a stationary state within the first hundred MC steps.

A. Structural properties

The aim of the first part of the analysis is to explore the phase diagram of the tissues using as control parameters the target shape parameter p_0 and the temperature T. As structural order parameter we measure the average observed shape parameter q, since as explained above it determines the state (solid or liquid) of the system. Our study will be around the critical point $q^* \approx 3.81$ hence following [2] p_0 will take values in $[3, 4]$. This limits the range of temperatures that allows us see a solid-to-liquid transition, which will be $(0, 0.1)$ (notice that if temperature is too high then Eq.(6) approaches 1 and therefore every trial move is accepted). As Fig.(2) shows, q fluctuates around a certain value, so we will consider the average of q over the last 300 steps as the one that determines the state of the system.

In Fig.(3) we have this averaged value of q represented for different conditions of temperature and p_0. It is worth noting that for most conditions of p_0 and T, q does not match the target p_0 (the dashed lined represents the identity line), which means that the system cannot dynamically satisfy the constraints imposed by the mechanical

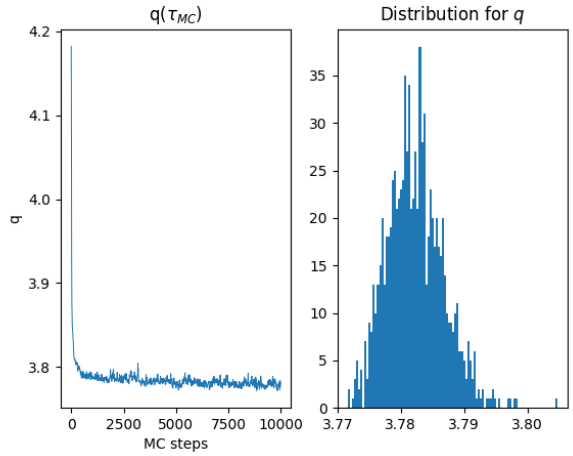

FIG. 2: Evolution of q over time in the left image and distribution of q (after termalisation) on the right, for $p_0 = 3.73$ and $T = 0.01$ As with energy, q quickly starts fluctuating in a small interval

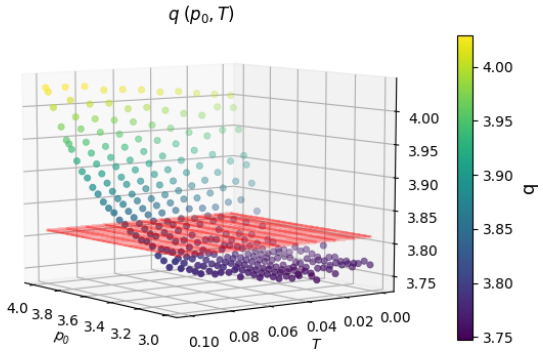

FIG. 4: Representation of q (color scale) for different conditions of temperature and p_0 in a 3D plot. The semi-transparent red plane is the constant value $q = q^* = 3.81$, and therefore the points below it correspond to a solid state and the points above it to a liquid.

energy, i.e., all cells with the same p_0. Therefore the system remains blocked at some configuration, which for low values of p_0 and T has $q \approx q^{hex}$. Taking the transition point from solid to liquid $q^* = 3.81$ we can find the state of every system in the phase space (p_0, T, q), obtaining the phase diagram in Fig.(4).

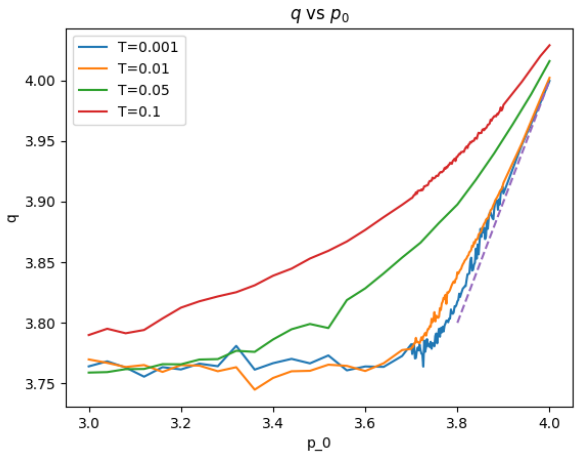

FIG. 3: Representation of the mean observed shape parameter q (averaged over the last 300 MC steps) versus the target shape parameter p_0, for different temperatures (error bars have not been included). The dashed line represents the identity function.

We can visually check these predictions in the examples in Fig.(5) (liquid state) and Fig.(6) (solid state). We can see that a solid shows a more homogeneous state, where cells are mostly regular hexagons ($q \approx 3.72$) and the shape parameter is approximately constant throughout the tissue. On the other hand, the liquid state displays a wider variety of polygons with 4,5 and 6 sides, and therefore the shape parameter is less uniform. In Fig.(7) we have tracked the trajectories of 10 arbitrary cells in a solid tissue (left) and liquid tissue (right). We clearly see that in a solid cells remain in a very bounded space, while in a liquid they are able to move.

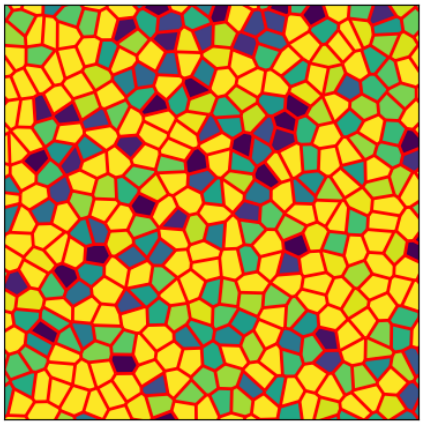

FIG. 5: Voronoi tesseletion of the final coordinates of the cells centers of a 400 cell tissue with temperature 0.08 and $p_0 = 3.9$ (liquid state) with the same color scale as Fig.(4)

B. Dynamical properties

We start with studying the mean squared displacement, which is defined as

$$\Delta r^2(t) = \frac{\sum_{cells\ i} (\mathbf{r}_i(t) - \mathbf{r}_i(0))^2}{N}$$

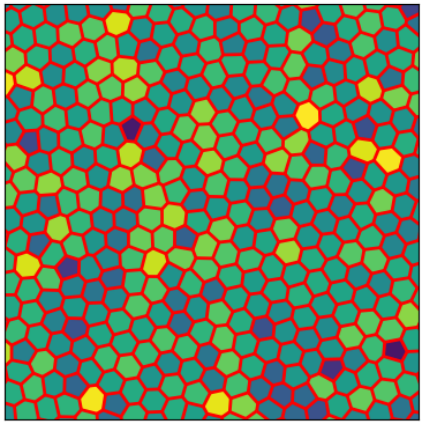

FIG. 6: Final snapshot of a tissue of 400 cells with temperature 0.02 and $p_0 = 3.2$ (solid state) with the same color scale as Fig.(4)

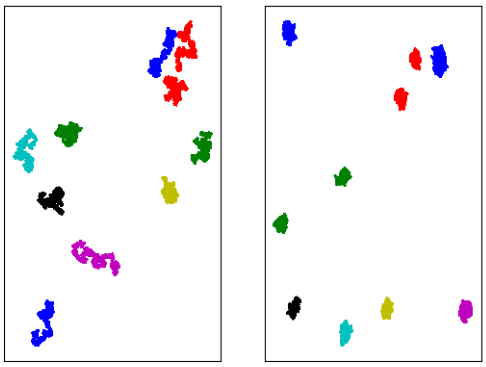

FIG. 7: Coordinates of the cells centers of 10 arbitrary cells for the last 1000 MC steps, the left figure for $p_0 = 3.8$ and $T = 0.08$ (liquid state) and the second one $p_0 = 3.2$ and $T = 0.02$ (solid state).

where $\mathbf{r}_i(0)$ is the position of the i-th cell center after termalisation. In Fig.(8) we see a representation of the mean squared displacement over time for different simulations. As we can see it exhibits a dependence on both, temperature and shape index. For liquid states it shows a linear dependence on t (diffusive regime). When approaching the transition we observe a subdiffusive regime ($\Delta r^2 \propto t^\mu$ with $0 < \mu < 1$) in between, and for solids we see diffusive-subdiffusive, where the subdiffusive regime develops a plateau. The plateau indicates that cells are being caged by their neighbours [2].

We can thus define the effective diffusion constant

$$D_{eff} = \lim_{t\to\infty} \frac{\Delta r^2}{4t}.$$

D_{eff} is measured from the final value the mean squared displacement. In Fig.(9) we see that for low values of p_0 D_{eff} is (almost) zero, until at a certain value of p_0 it

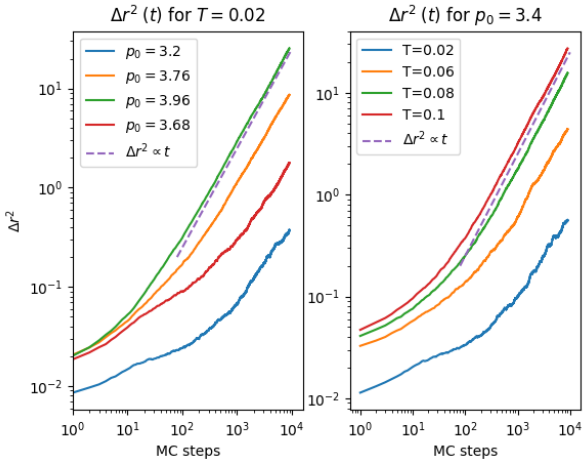

FIG. 8: Representation of the mean squared displacement over time for different conditions of p_0 and q. We have also represented a line with slope 1 (in log-log scale) that represents a diffusive regime.

becomes non-zero. Since the states with non-zero diffusion coefficient correspond to liquid states whereas solids have zero diffusion constant, we have obtained another way to determine the state of the tissue [2]. If we take this critical value of transition and represent it in the $p_0 - T$ plane (Fig.(10)) we see that it matches remarkably well with the transition points that we obtain if we take the systems in the phase diagram with $q \approx q^*$. As a matter of fact, the critical value of q obtained in this section is $q = 3.82 \pm 0.03$.

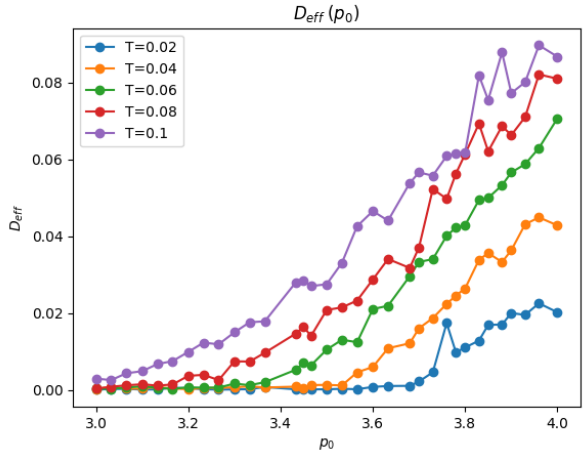

FIG. 9: Representation of the dependence D_{eff} (p_0) for different temperatures.

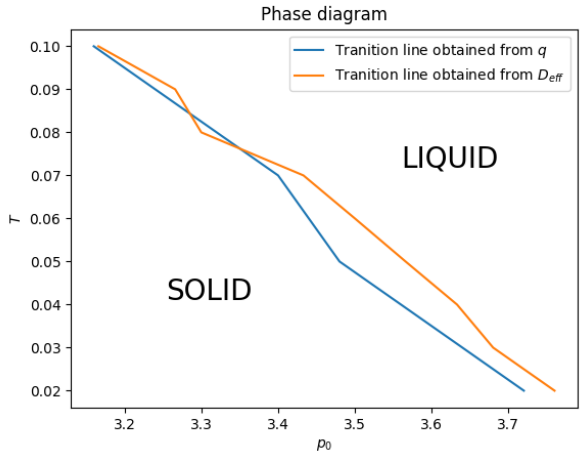

FIG. 10: Representation of the coordinates (p_0, T) by which D_{eff} starts having a non-zero value (orange line) and of the coordinates that lay on the plane $q = q^*$ in Fig.(4) (blue line), i.e., the transition points in the structural study. The blue points have an error on p_0 of ≈ 0.04, while for the red points the error is ≈ 0.03. As one can see, the two methods provide compatible results.

IV. CONCLUSIONS

We have explored the structural and dynamical properties of biological tissue in the framework of Voronoi models. We have considered a model of biological tissue where cells randomly move because of a thermal-like noise and studied the equilibrium states using the Monte Carlo method. Using as control parameters the shape index p_0, which measures the typical cell elongation, and the temperature T, which measures the strength of the noise, we have developed a phase diagram of the tissue that counts two phases: a solid state where cells do not move, and a liquid state where cells move. We can summarize our results as follows:

- The solid-liquid transition can be individuated using the structural order parameter q, which is a dimensionless relation between cells area and perimeter and separates solid states from liquid states at a critical value $q* \approx 3.81$.
- The same transition can be studied by looking at the long-time behavior of the mean-square displacement, which leads us to define a parameter that is non-zero for liquids and zero for solids.
- The transition line obtained by the two methods are consistent, and we reach the same critical value of the structural parameter from the dynamical approach.

Acknowledgments

I would like to thank the advisor of this project Dr. Matteo Paoluzzi for the excellent help and guidance he has provided me. To my parents, family and friends for giving me such a great years.

[1] Dapeng Bi, J. H. Lopez, J. M. Schwarz, and M. Lisa Manning. A density-independent rigidity transition in biological tissues. *Nature Physics*, 11:1074–1079, 2014.

[2] Dapeng Bi, Xingbo Yang, M. Cristina Marchetti, and M. Lisa Manning. Motility-driven glass and jamming transitions in biological tissues. *Phys. Rev. X*, 6:021011, Apr 2016.

[3] Dirk Dormann and Cornelis J Weijer. Chemotactic cell movement during development. *Current Opinion in Genetics and Development*, 13(4):358–364, 2003.

[4] Peter Friedl and Darren Gilmour. Collective cell migration in morphogenesis, regeneration and cancer. *Nature Reviews Molecular Cell Biology*, 10(7):445–457, July 2009.

[5] Peter Friedl and Roberto Mayor. Tuning collective cell migration by cell-cell junction regulation. *Cold Spring Harbor perspectives in biology*, 9 4, 2017.

[6] Hisao Honda. Description of cellular patterns by dirichlet domains: The two-dimensional case. *Journal of Theoretical Biology*, 72(3):523–543, 1978.

[7] Denise Montell. Border-cell migration: The race is on. *Nature reviews. Molecular cell biology*, 4:13–24, 02 2003.

[8] Matteo Paoluzzi, Luca Angelani, Giorgio Gosti, Marchetti, et al. Alignment interactions drive structural transitions in biological tissues. *Phys. Rev. E*, 104:044606, Oct 2021.

[9] Jin-Ah Park, Jae Hun Kim, Dapeng Bi, Jennifer A Mitchel, et al. Unjamming and cell shape in the asthmatic airway epithelium. *Nature Materials*, 2015.

[10] M. Poujade, E. Grasland-Mongrain, A. Hertzog, J. Jouanneau, et al. Collective migration of an epithelial monolayer in response to a model wound. *Proceedings of the National Academy of Sciences*, 104(41):15988–15993, 2007.

[11] Raimon Sunyer, Vito Conte, Jorge Escribano, et al. Collective cell durotaxis emerges from long-range intercellular force transmission. *Science*, 353(6304):1157–1161, 2016.

[12] Xavier Trepat and Erik Sahai. Mesoscale physical principles of collective cell organization. *Nature Physics*, 14(7):671–682, July 2018.